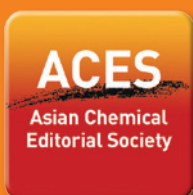


# ASIAN JOURNAL OF ORGANIC CHEMISTRY

www.AsianJOC.org



A Journal of



# REPRINT

WILEY-VCH

# Nucleophilic Addition to Diradicals Derived From Cycloaromatization of Maleimide-Based Eneidyne

Mengsi Zhang, Hailong Ma, Baojun Li, Ke Sun, Haotian Lu, Wenbo Wang, Xiaoyu Cheng, Xiaoxuan Li, Yun Ding,\* and Aiguo Hu\*<sup>[a]</sup>

**Abstract:** Diradical chemistry, typified by the cycloaromatization of enediynes or enyne-allenes, have been extensively explored due to the involved intriguing biological activity and unique mechanistic actions. Because of the essential Myers-Saito cycloaromatization involved in the maleimide-assisted rearrangement and cycloaromatization (MARACA) mechanism disclosed in our recent work, the important object of diradical/zwitterion dichotomy and the reactivity of thermally induced  $\sigma,\pi$ -diradicals were investigated in this work through the combination of experimental and computational studies. Deuterium incorporation experiments demonstrated that the polar product was afforded from the MARACA strategy, in which the diradical and zwitterion

reactivities from the cycloaromatization step could both lead to the closed-shell product via the subsequent nucleophilic addition reaction and protonation. Using the density functional theory calculations, the unusual reactivity of the heterosymmetric diradicals to closed-shell zwitterions was examined, and the addition of carbonyl moiety to  $\alpha,3$ -dehydrotoluene was allowed to occur via a nonplanar cyclic allene transition structure with a small barrier of 9.1 kcal/mol. The observed nonplanar geometry is essential for the necessarily symmetry-breaking action, resulted in the continuous transformation from open-shell diradical to closed-shell zwitterion species during the addition process.

## Introduction

Cycloaromatization reactions, typically exemplified by Bergman cyclization (BC)<sup>[1]</sup> and Myers-Saito cyclization (MSC),<sup>[2]</sup> are intriguing in the chemistry of enediynes or enyne-allenes. The special feature of cycloaromatization for both cases lies at the creation of one  $\sigma$ -bond and two radical centres with the sacrifice of two  $\pi$ -bonds as a result of transforming the closed-shell molecules into reactive diradical species.<sup>[3]</sup> The generated reactive centres are beneficial for many perspectives in organic synthesis,<sup>[4]</sup> drug discovery<sup>[5]</sup> and materials science.<sup>[6]</sup> For example, the 1,4-benzene diradicals formed through BC process under biological conditions account for a fascinating class of naturally occurring enediyne antibiotics like Calicheamicins,<sup>[7]</sup> Dynemicins,<sup>[8]</sup> and Esperamicins<sup>[9]</sup> with astounding bioactivity for antitumor applications.<sup>[10]</sup> In addition, the important biological performance of another kind of natural products like neocarzinostatin (NCS)<sup>[11]</sup> attributes to the potential of diradicals derived from MSC of enyne-allene moiety. Besides BC and MSC, many related reactions that transform closed-shell molecules into diverse diradical systems continue to expand on the way, including Schreiner-Pascal,<sup>[12]</sup> Schmittel,<sup>[13]</sup> Garratt-Braverman,<sup>[14]</sup> Hopf,<sup>[15]</sup> and Moore<sup>[16]</sup> cyclization reactions. The promising

future of cycloaromatization theme triggering radical production from closed-shell precursors encourages one to further explore the curious world of diradical chemistry.

Nevertheless, the general principle where the choice between the nonpolar and polar extremes exists every time when a chemical bond is broken, unsurprisingly endows the formed intermediates with the dual reactivity in the cycloaromatization, behaving either in a diradical or a zwitterion form.<sup>[3,17]</sup> Indeed, there has been emerging evidences of extending to the formation of zwitterions beyond diradicals when the cycloaromatization proceeds under suitable reaction conditions, such as in the presence of Au(I) catalysts,<sup>[18]</sup> nucleophilic solvents<sup>[19]</sup> or specific substituents.<sup>[20]</sup> Alabugin et al. have summarized the unusual chemistry and paid special attention to the dichotomy between diradical and zwitterionic species.<sup>[3,17]</sup> Among these, the dichotomy of two species within many kinds of cycloaromatizations has invoked intriguing mechanistic discussion. For example, Myers and co-workers originally assigned the presence of a resonance structure between the open-shell diradical and the closed-shell zwitterion to the formation of the corresponding radical and ionic products, which however was disagreed by Carpenter et al. because the mixing of two electrons is symmetry forbidden in the heterosymmetric Myers-Saito  $\sigma,\pi$ -diradicals.<sup>[21]</sup> They further suggested that a nonadiabatic surface crossing from the ground-state reactant to the excited-state zwitterion intermediate occurred after the transition structure during the cycloaromatization process, indicating the existence of two parallel mechanisms in which the zwitterionic intermediate was responsible for the unexpected polar products.<sup>[22]</sup>

Apart from the directly formed zwitterionic species from the substrates, an alternative path where the nucleophilic addition

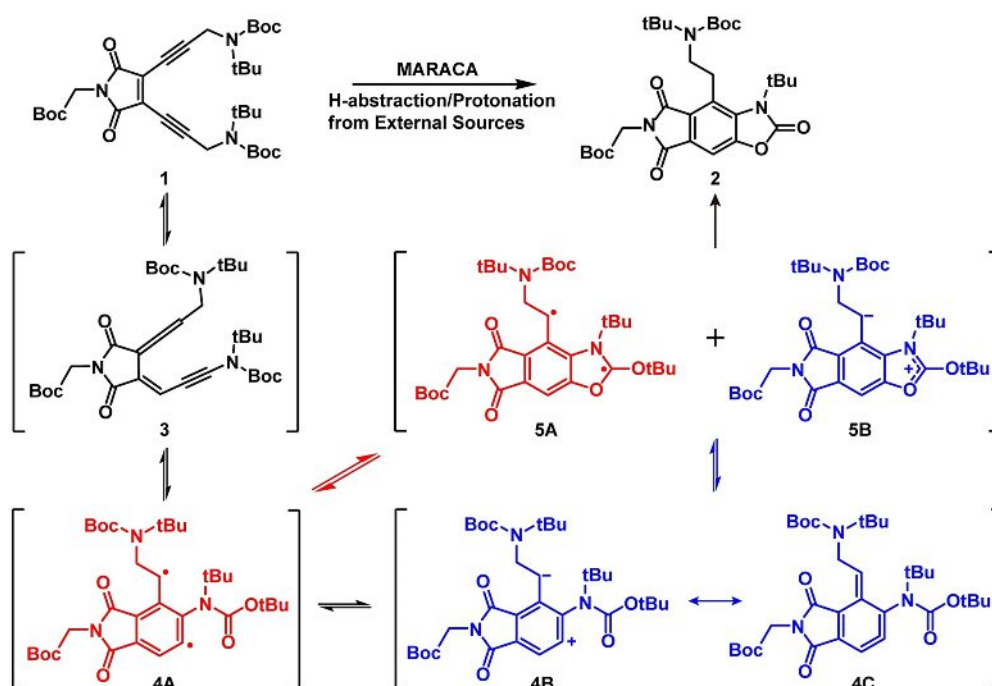
[a] M. Zhang, H. Ma, B. Li, K. Sun, H. Lu, W. Wang, X. Cheng, X. Li, Dr. Y. Ding, Prof. Dr. A. Hu  
Shanghai Key Laboratory of Advanced Polymeric Materials, School of Materials Science and Engineering  
East China University of Science and Technology  
Shanghai 200237 (P. R. China)  
E-mail: yunding@ecust.edu.cn  
hagmhsn@ecust.edu.cn

Supporting information for this article is available on the WWW under <https://doi.org/10.1002/ajoc.202100136>

to diradicals after the cycloaromatization step has been manifested to be accessible to the polar products. Generally, the ionic reactivity in neutral systems is unfavorable owing to the involved charge separation process. As a consequence, the case of nucleophilic addition to homsymmetric  $\sigma,\sigma$ -diradicals derived from BC was firstly reported until 2007 by Perrin et al.<sup>[23]</sup> Recently, Basak et al. have reported the similar studies on nucleophilic addition reactions on several enediyne, affording deeper understanding of the ionic chemistry of the p-benzynes intermediate.<sup>[24]</sup> Subsequently, Winter et al. demonstrated that the addition of nucleophiles to homsymmetric diradicals can proceed without any symmetry restrictions or reaction barrier according to the high-level multireference computations.<sup>[25]</sup> Similarly, they investigated the addition process to heterosymmetric diradicals as a representative of intermediates produced from MSC of enyne-allenes.<sup>[26]</sup> Unlike the former case, a nonplanar cyclic allene geometry has been illustrated during the approach of a chloride ion to the radical center because the intrinsic orbital symmetry is broken upon the addition process. Thus, these theoretical results may provide an explanation of the addition product observed in the reaction of  $\alpha,3$ -dehydrotoluene formed from MSC with methanol.<sup>[2a,b]</sup> Different from the former cases in which the external nucleophiles were needed, certain substitution could also behave like the "intramolecular nucleophilic reagent", inducing the switch from diradicals to zwitterions through the orbital isomerization in a special case of Moore cyclization.<sup>[20a]</sup>

In our early efforts of exploring the maleimide-based acyclic enediyne with potent antitumor activity, the cycloaromatization reactivity of enediyne was manipulated regarding to the steric and electronic effects of substitutions in the terminal

alkyne.<sup>[27]</sup> Following this line, a new mechanism named as maleimide-assisted rearrangement and cycloaromatization (MARACA) to trigger the antitumor potency of enediyne was proposed recently.<sup>[28]</sup> Moreover, the interception pathways by intramolecular hydrogen atom transfer (HAT) with regard to highly reactive diradicals generated through MARACA have been uncovered,<sup>[29]</sup> which clearly indicated that the intramolecular HAT pathways to consume the diradical species have posed a challenge to further boost their biological activity unless the enediyne molecules are elaborately designed. On the other hand, because of the involvement of the essential MSC step in the MARACA mechanism, the dual reactivity of the intermediates from cycloaromatization is expected to show up. Looking back at the MARACA of enediyne such as compound 1 (Scheme 1), we reconsider the possible pathways toward the isolated compound 2. According to the dichotomy in cycloaromatization, both the reactive diradical 4A and zwitterion 4B intermediate can be formed from the MSC of the transient enyne-allene 3. After the specific 5-endo cyclization, the pathways of the H-abstraction by 5A and the protonation of 5B both lead to the identical structure of compound 2. In principle, it is possible for the carbon radical center in 4A to exhibit the zwitterionic (4B) or/and electrophile (4C) character via orbital isomerization upon the attack by the adjacent carbonyl group.<sup>[30]</sup> Notably, the manner of 5-endo attack in 4A leading to 5A or 5B determines if the diradicals will be quenched or not. To resolve these issues, the three modes of reactivities (4A, 4B and 4C) accessible to generate the product 2 after MARACA process are investigated experimentally and computationally in this work. Of special note is that the carbonyl group within molecule itself could behave as a "nucleophile", resulted in the



**Scheme 1.** The rearrangement and cycloaromatization of maleimide-based enediyne 1 and the subsequent 5-endo attack induced orbital isomers leading to the formation of compound 2.

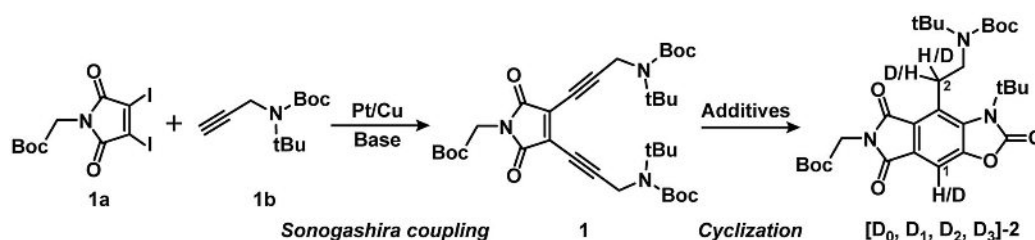
switch from diradicals to zwitterionic species. Considering the nucleophilic addition to heterosymmetric  $\sigma,\pi$ -diradicals, the configuration change from open-shell to closed-shell species would be allowed unless the symmetry of the system is broken.<sup>[31]</sup> As expected, the nonplanar cyclic allene geometry as the transition structure is involved along the addition reaction, in which the unimolecular addition process is similar to that of the reaction of  $\alpha,3$ -dehydrotoluene with an additional nucleophile.<sup>[26]</sup>

## Results and Discussion

**Radical and ionic pathways toward compound 2 after MARACA.** In our previous investigation on the MARACA mechanism,<sup>[28]</sup> the transformation of enediyne **1** into the cyclized product **2** was not only observed after its being heated in methanol at 37 °C but also found during the synthesis of enediyne **1** under the Sonogashira coupling conditions (Scheme 2). The possible reaction pathway from compound **1** to **2** has been suggested, but the key issue concerning the determination of radical and/or ionic pathways after cycloaromatization of the enyne-allene precursor **3** was not clarified. To gain a deeper insight into this process, several control experiments using the additives serving as the hydrogen atom or proton donors were carried out. The compound **2** was obtained in a moderate yield through this tandem Sonogashira coupling/cyclization processes. The one-pot synthesis accompanying with deuterated agents to be added directly into the system was adopted with no need to isolate compound **1**, leading to the distinct products of deuterium incorporation into compound **2** (Scheme 2). The results of the product distribution bearing varied numbers of deuterium atoms are summarized in

Table 1, evaluated from both nuclear magnetic resonance (NMR) and high-resolution mass spectrometry (HRMS) analysis.

When mixed additives of 10 eq CD<sub>3</sub>OD and 4 eq D<sub>2</sub>O were applied in the one-pot reaction, significant incorporation of deuterium at C-1 (phenylic position) and C-2 (benzylic position) were observed from the NMR peak integration analysis (entry 1, Table 1). As suggested in the MARACA mechanism,<sup>[28]</sup> the incorporation of the deuterium at C-1 and the first deuterium at C-2 could be achieved during the cascade rearrangement processes for generating the MSC precursor **3**. Therefore, the presence of [D<sub>3</sub>]-**2** (13.6%) with three deuterium atom incorporation indicated the occurrence of H-abstraction/protonation after the cycloaromatization from deuterium atom and/or ion donors CD<sub>3</sub>OD/D<sub>2</sub>O. In order to disclose which path dominates, control experiments with only deuterium-ion donors (entry 2 and 3, Table 1) or only deuterium-atom donors (entry 4, Table 1) were performed under the same condition. The use of CH<sub>3</sub>OD/D<sub>2</sub>O or CH<sub>3</sub>OD led to similar deuteration distributions with that of CD<sub>3</sub>OD/D<sub>2</sub>O. By contrast, no deuterated **2** was formed in the case of CD<sub>3</sub>OH/H<sub>2</sub>O. The same experimental sets were extended to (CD<sub>3</sub>)<sub>2</sub>CDOD/D<sub>2</sub>O and (CD<sub>3</sub>)<sub>2</sub>CDOH/H<sub>2</sub>O systems. Both cases were in good accordance with the above observation that the high deuteration degree was afforded for protic deuterated agents (entry 5, Table 1), while non-deuterated product for the other case (entry 6, Table 1). The deuterium incorporation experiments were also performed with pure compound **1** to avoid the influence of other additives added for Sonogashira reaction. After incubated in CH<sub>3</sub>OD or CD<sub>3</sub>OH at 37 °C till the complete consumption of compound **1**, the mixtures were subjected for HRMS analysis, showing similar deuterated product distribution (Table S1). Altogether, these results indicate that the presence of protic additives is crucial for the deuterium incorporation into compound **2**. Although the radical relevant reactivity of deuterium abstraction from



Scheme 2. One-pot synthesis for the deuterium incorporation into compound **2** in the presence of deuterated additives.

Table 1. The deuterium incorporation into compound **2** in the presence of different additives.

entry	Additives <sup>[a]</sup>	NMR <sup>[b]</sup>		HRMS <sup>[c]</sup> 0D	1D	2D	3D
		C-1	C-2				
1	CD <sub>3</sub> OD/D <sub>2</sub> O	0.32	1.06	15.0%	35.9%	35.6%	13.6%
2	CH <sub>3</sub> OD/D <sub>2</sub> O	0.33	1.08	5.8%	35.3%	52.2%	6.7%
3	CH <sub>3</sub> OD	0.39	1.24	9.0%	41.7%	43.4%	5.9%
4	CD <sub>3</sub> OH/H <sub>2</sub> O	1	2	100.0%	0	0	0
5	(CD <sub>3</sub> ) <sub>2</sub> CDOD/D <sub>2</sub> O	0.31	1.03	12.5%	36.4%	40.1%	11.0%
6	(CD <sub>3</sub> ) <sub>2</sub> CDOH/H <sub>2</sub> O	1	2	100.0%	0	0	0

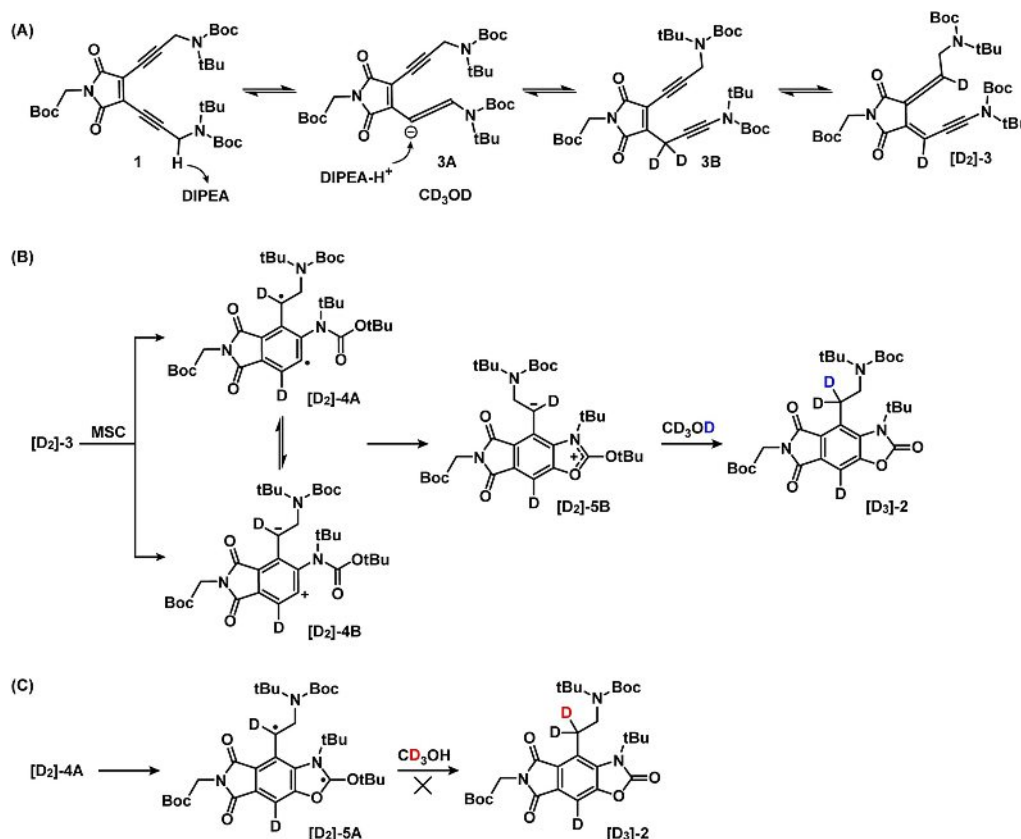
[a] The equivalent of additives: alcohol/water (10/4). [b] The residual integration of proton signals at C-1 or C-2 position in NMR. [c] The products distribution calculated by ESI-HRMS analysis for the mixtures.

C–D of alcohols (entry 4 and 6, Table 1) was not detected, the radical mode cannot be ruled out because of the shift to the ionic path when CD<sub>3</sub>OH was used as the hydrogen donor as observed by Myers.<sup>[2b]</sup>

The plausible pathways toward compound [D<sub>3</sub>]-2 are described in Scheme 3, which reasonably accounts for the varied reactivities of deuterium observed. For the case of additives bearing polar deuterium, the base-assisted cascade proton migration processes of enediyne compound 1 occur, resulted in the deuterium labeled [D<sub>2</sub>]-3 (Scheme 3A). Subsequently, this MSC precursor undergoes cycloaromatization to give diradical [D<sub>2</sub>]-4A and zwitterionic [D<sub>2</sub>]-4B intermediates, in which one deuterium locates at the phenylic site while the other at the benzylic position. Considering the failure of deuterium incorporation into compound 2 with deuterium-atom only donors (entry 4 and 6, Table 1), the path of deuterium abstraction by benzylic radical to [D<sub>3</sub>]-2 should be unfeasible (Scheme 3C). Therefore, the second benzylic deuterium would be only from the O–D positions of alcohols via the possible zwitterionic species [D<sub>2</sub>]-5B (Scheme 3B). Due to the higher reactivity imparted by phenylic reactive center compared to the benzylic one, the key intermediate [D<sub>2</sub>]-5B is expected to yield upon the 5-endo attack to either [D<sub>2</sub>]-4A or [D<sub>2</sub>]-4B before the protonation of benzylic position. Indeed, it is easily accepted that the nucleophilic addition of carbon cation by the carbonyl group would maintain the zwitterionic reactivity, and

eventually generate the desired polar product [D<sub>3</sub>]-2 followed by protonation and the leaving of tert-butyl cation. On the other hand, the possibility of the nucleophilic attack to  $\sigma$ -radical center intramolecularly by electron-rich carbonyl group for the formation of [D<sub>2</sub>]-5B deserves to disclose since several cases have demonstrated that the nucleophilic addition to diradicals could proceed in the presence of additional halide nucleophiles.<sup>[23,32]</sup> Together with the reported experimental and computational evidence, although the intramolecular nucleophilic path exist, the  $\alpha,3$ -dehydrotoluene derived from cycloaromatization of enediynes are also likely trapped by external nucleophiles like halides. Currently, the unusual path proposed for the formation of [D<sub>2</sub>]-5B cannot be directly concluded from experimental data, hence we turn to computational study for further clarification.

**Computational study.** Notably, the conversion of closed-shell enediyne compound 1 to open-shell diradical species 4A containing cascade rearrangement and cycloaromatization processes have been investigated by our previous computational study.<sup>[28]</sup> Herein, we mainly focused on the following courses, especially for the evolution of diradical 4A to closed-shell 5B along the proposed reaction path. Density functional theory (DFT)<sup>[33]</sup> calculations were conducted in the Gaussian 09 package<sup>[34]</sup> at the UB3LYP/6-31G\* level in the gas phase, in which the structurally simplified models were used to test the hypothesis (Figure 1). The B3LYP functional along with the



**Scheme 3.** Plausible pathways toward compound [D<sub>3</sub>]-2 in the presence of CD<sub>3</sub>OD or CD<sub>3</sub>OH for the sequential reaction. (A) The involved cascade rearrangement processes starting from compound 1. (B) The MSC of enyne-allene [D<sub>2</sub>]-3 and the following 5-endo cyclization before protonation to give [D<sub>3</sub>]-2. (C) The inaccessible path to [D<sub>3</sub>]-2 via [D<sub>2</sub>]-5A in the presence of CD<sub>3</sub>OH.

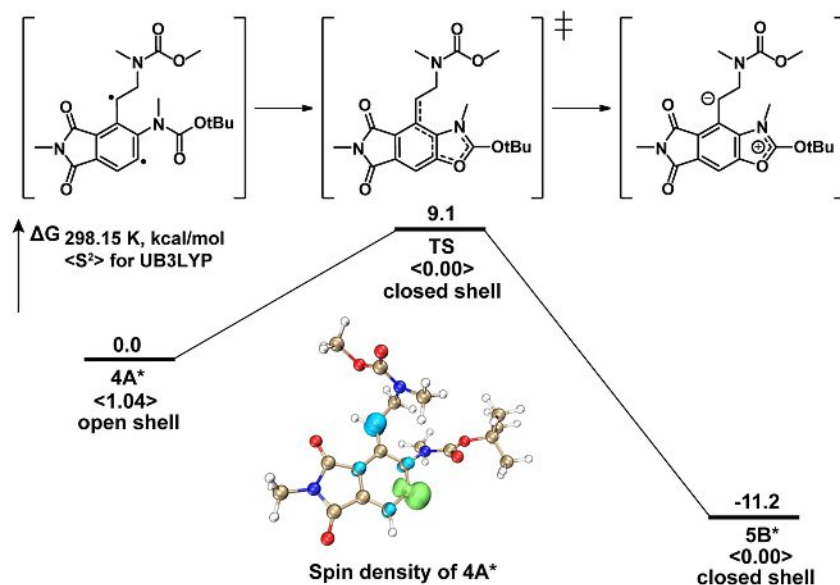


**Figure 1.** A computational study on the reactivity of diradical **4A\***. Gibbs free energy profile (kcal/mol) calculated at UB3LYP/6-31G(d) level. Inset is the spin density plot for the  $\sigma,\pi$ -diradical intermediates **4A\***.

medium 6-31 g(d) basis set is suited for the application in the diradical systems calculations.<sup>[35]</sup> As for the addition of the nucleophilic moiety to the diradicals, the unrestricted broken-symmetry method with the keyword of “guess=(mix, always)” has been employed in the calculations with the consideration of the possible open-shell character of the electronic state for the optimized geometries. The approach was suited for the radical character analysis of heterosymmetric diradicals,<sup>[26]</sup> and the resulting value of  $\langle S^2 \rangle$  is very close to 1.0 for a pure diradical. In addition, intrinsic reaction coordinate (IRC) calculations were performed to confirm the connection of each TS to the minima of reactant and product. To further explore solvent effects, IRC calculations were also conducted employing a polarizable continuum model (PCM)<sup>[36]</sup> for toluene, tetrahydrofuran (THF),  $\text{CH}_3\text{OH}$ , and  $\text{H}_2\text{O}$ .

As shown in Figure 1, the calculations reveal a low-energy-demanding 5-endo cyclization route with a barrier of 9.1 kcal/mol. In this case, the typical  $\sigma,\pi$ -diradical character of **4A\*** as depicted from spin density distribution and the expected value of  $\langle S^2 \rangle$  (1.04) is indicated. However, both the optimized structures of **TS** and **5B\*** were shown in closed-shell forms. The energy of the triplet state for the diradical structure **4A\*** was also calculated, and it is only 0.7 kcal/mol higher than that of singlet state, thus indicating that the triplet state would not affect the addition pathways present. Unlike the observation of the barrierless addition to  $\alpha,3$ -dehydrotoluene with chloride ion in Winter’s work,<sup>[26]</sup> the Gibbs free energy barrier presented here may arise from the creation of charge separation along the cyclization path from the neutral system or the broken aromaticity required (discussed below). Moreover, the placement of nucleophilic and electrophilic reactivity in **5B\*** could be determined from the molecular orbital calculations. For example, the distribution of the highest occupied molecular orbital (HOMO) indicated that the carbon atom at benzyl position has

the high reactivity with electrophile. Likewise, the nucleophilic position is predicted in newly formed five-membered ring moiety according to the lowest unoccupied molecular orbital (LUMO) (Figure 2). In fact, in comparison with the typical zwitterionic intermediate derived from MSC, the unprecedented umpolung for the formation of benzylic anion and endocyclic cation in maleimide-based enediyne was offered, which has also been observed in the bromide addition product in our previous work.<sup>[32b]</sup> We believe that the stabilization of the endocyclic cation by adjacent heteroatoms in this case as well as the important effect given by electron-withdrawing group (maleimide moiety) for the benzylic anion may be responsible for these kind of interesting polar species.

Another special interest revealed by the calculations is that how the unimolecular addition process shifting the otherwise open-shell diradical species to the closed-shell product is allowed to occur without the assistance from external additives, eventually resulting in the  $\sigma,\pi$ -mixing in **5B\***. In principle, the transformation of heterosymmetric  $\alpha,3$ -dehydrotoluene diradicals to the coupled electronic structures could be accessible via orbital isomers when the original orbital symmetry of the

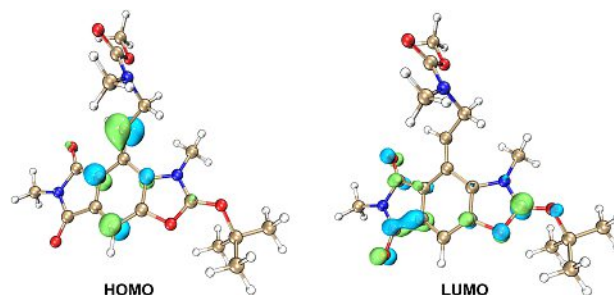


**Figure 2.** Molecular orbital plots of **5B\*** as determined from UB3LYP/6-31G(d) calculations.

system is broken,<sup>[31,37]</sup> which would involve the distorted geometries along the addition reaction. Thus, the  $\alpha,3$ -dehydrotoluene ring planarity of the involved geometries was investigated (Figure 3). As expected, both diradical **4A\*** and zwitterion **5B\*** displayed a near-planar geometry with measured dihedral angle no more than  $15^\circ$  between the selected planes. In contrast, the benzene ring in the TS exhibited pronounced pucker, implying a cyclic allene character (**4C\***), consistent with the reaction taking place via orbital isomer **4B\*/4C\*** (Scheme 4). Another two dihedral angles concerning benzene ring planes for each structure were given in Figure S1, confirming the highly bended structure in **4C\***. On the basis of the calculation results, we conclude that the nucleophilic addition of carbonyl group to planar  $\alpha,3$ -dehydrotoluene leading to the zwitterion **5B\*** proceeds via a closed-shell nonplanar transition state, where **4** might also act as the electrophile apart from the diradical and zwitterion mode of reactivity. The dual zwitterionic/electrophilic reactivity likely provided the access to the formation of compound **2**.

Apart from the mentioned case of nucleophilic addition to diradicals, the suggested alternative pathway toward **5B\*** involving the cyclic-allene-like structure **4C\*** was indeed not well recognized yet.<sup>[26]</sup> Especially in this case, it was promoted by the unique intramolecular addition where the carbonyl group within the molecule behaved as the nucleophile. As for the significant switch from open-shell to the closed-shell configurations, the evolution of the electronic structures and the radical character during the addition process needs to be paid special attention. To characterize the changing of the diradical character along the IRC for the addition reaction, the  $\langle S^2 \rangle$  values were examined, and that values of approximately 1.0 can be taken as a marker for perfect diradicals.<sup>[38]</sup> Contrary to the sharply increased  $\langle S^2 \rangle$  values from 0.0 to 1.0 just after

the TS point in MSC (Figure 4A), a gradual and continuous decrease of  $\langle S^2 \rangle$  to 0.0 at TS point was shown in the 5-endo cyclization (Figure 4B), suggesting the completely disappeared diradical character starting from the TS in the latter case. This evolution of the diradical character disclosed the generation of diradical species via MSC and the subsequent interception by nucleophilic addition to afford the closed-shell zwitterion **5B\***. Meanwhile, a description of the change in geometries along the addition is given in Figure 4B, showing as the change from black to red squares. As expected, the diradical reactant (**4A\***) along with the zwitterion product (**5B\***) exhibit planar geometries, but the mix of two distinct electronic states were allowed to occur via nonplanar geometries due to the required symmetry breaking for  $\alpha,3$ -dehydrotoluene diradicals. Overall, the thermally induced MSC resulted in the formation of  $\alpha,3$ -dehydrotoluene derivative, whose diradical reactivity likely led to unexpected polar products via nonplanar reaction pathway.

As for the diradical/zwitterion dichotomy in  $\alpha,3$ -dehydrotoluene chemistry, there is increasing evidence that a marked preference of the zwitterionic to radical pathway under polar conditions or nucleophilic solvents, as supported by computational and experimental approaches.<sup>[19,39]</sup> But unlike the previous work, the nucleophilic addition to phenylic radical position in this work performed as a unimolecular process, shifting the diradical to closed-shell polar product. To explore if the diradical/zwitterion switch was sensitive to the polarity of environment, the  $\langle S^2 \rangle$  values along the IRC were computed in toluene ( $\epsilon = 2.37$ ), THF ( $\epsilon = 7.42$ ), methanol ( $\epsilon = 32.61$ ) and water ( $\epsilon = 78.35$ ) (Figure 5). Remarkably, the diradical character diminished gradually to 0.0 at TS point. Then, the geometries maintained an  $\langle S^2 \rangle$  value of 0.0 after the TS in all the tested media, consistent with that observed in the gas phase, exhibiting negligible change as solvent dielectric constant

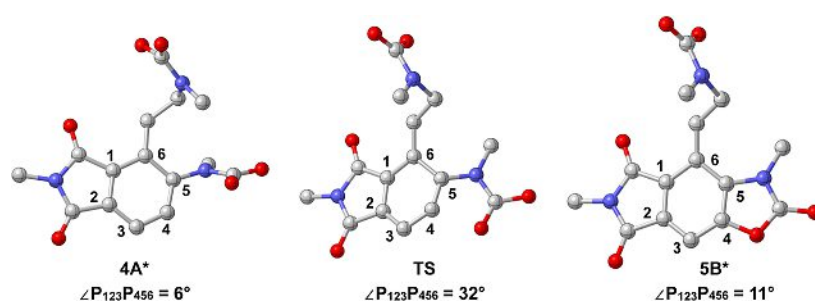
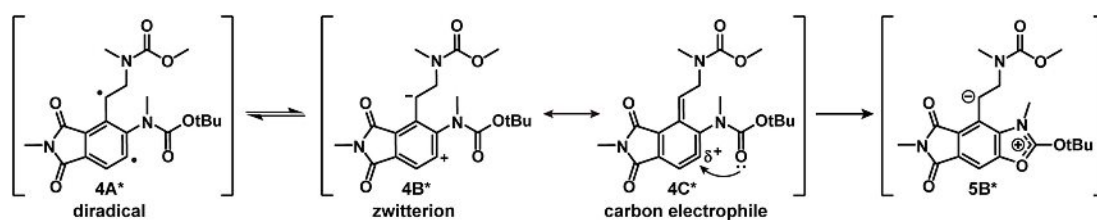


**Figure 3.** Observed high planarity in diradical **4A\*** and zwitterion **5B\*** contrasts with the pronounced puckered geometry of TS along the reaction path shown in Figure 1. Geometries simplified for clarification.  $P_{123}$  or  $P_{456}$  represents the plane constituted by the three adjacent atoms in benzene ring. The dihedral angles between concerned planes for each geometry are given.



**Scheme 4.** A computational study on the 5-endo cyclization triggering the diradical **4A\*** into zwitterion **5B\*** via a closed-shell transition state.

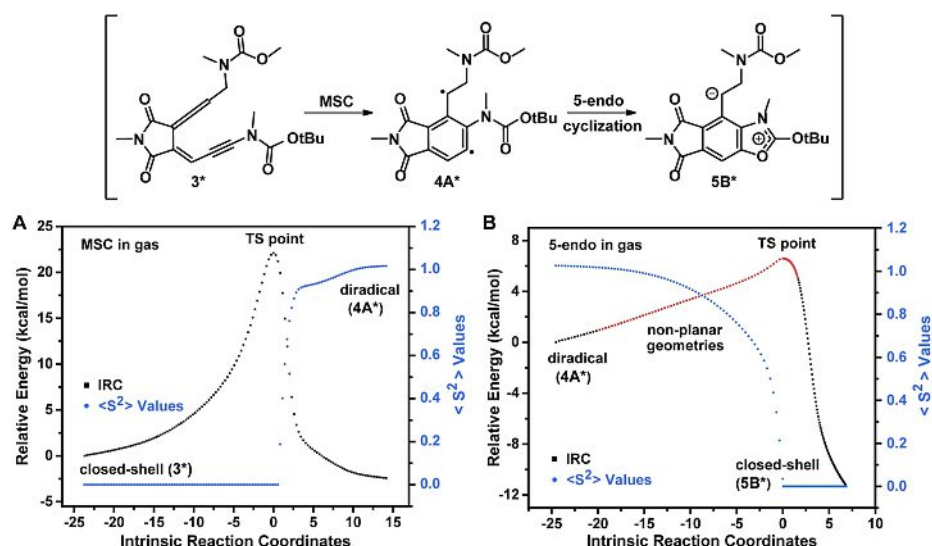


**Figure 4.** The  $\langle S^2 \rangle$  value progression along the reaction coordinates from closed-shell enyne-allenes  $3^*$  to diradical product  $4A^*$  via MSC (A), and the following 5-endo cyclization to regain the closed-shell specie  $5B$ . The red squares are the relative energy for nonplanar geometries (B).

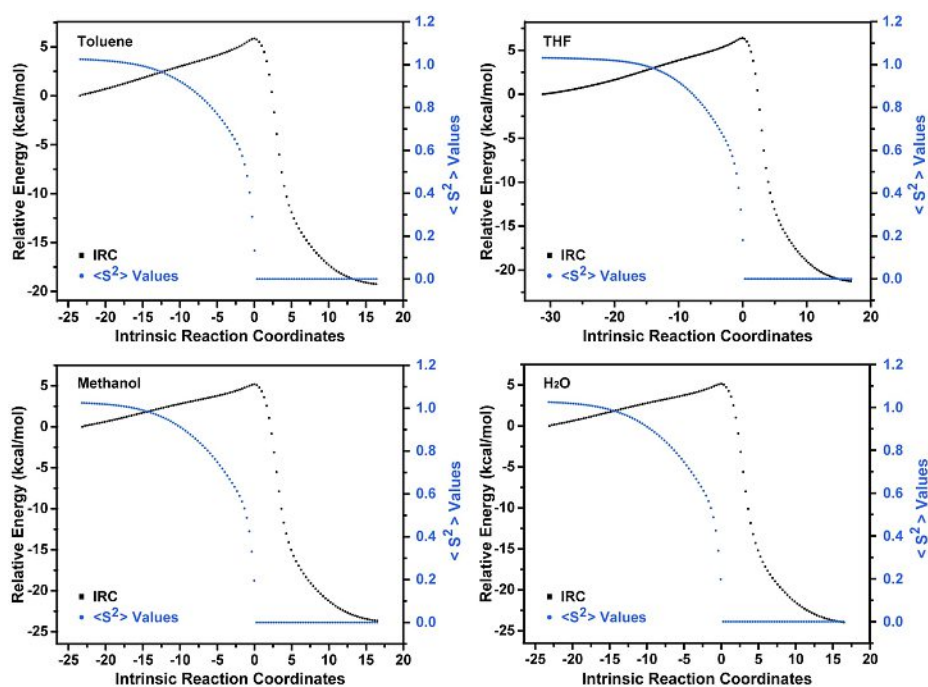


**Figure 5.** IRC plots for 5-endo cyclization of  $4A^*$  in various solvents. Relative energy (kcal/mol) and  $\langle S^2 \rangle$  values versus reaction coordinates are plotted.

increased. The continuous transition from the (planar) open-shell to (distorted) closed-shell geometry along the addition reaction clearly displayed solvent insensitivity. In addition, there was a small separation of charges on two radical carbon atoms along the IRC (Figure S2), which strengthened the above point that there was no polar electronic state involved in the present pathway. According to this result, we believe that the intramolecular nucleophilic addition process starting from radical to zwitterion product does not involve the polar electronic state, thus showing no significant solvent polarity dependence.

## Conclusion

In summary, intrigued by the newly discovered MARACA mechanism that involved the essential cycloaromatization reaction for the enediynes or enyne-allenes chemistry, we turn our attention to the diradical/zwitterion dichotomy in the cycloaromatization of maleimide-based enediynes that lead to the corresponding radical and polar products. In the deuterium-labelling experiment for the 5-endo cyclized H-abstraction product, the indication of polar rather than radical product was obtained. Although the direct D-abstraction from the C–D of

chosen alcohol has not been detected, the radical path leading to the identical compound cannot be firmly ruled out. The observed ionic product was likely generated from the zwitterion intermediate via MSC as usual. Alternatively, a unique diradical reactivity promoted by the nucleophilic addition responsible for the formation of polar product is proposed here. Theoretical calculations showed that the continuous transformation from the open-shell diradical to the closed-shell zwitterion could proceed via a nonplanar process, in which the twisted cyclic allene acts as the transition state. Again, the addition of carbonyl group to the phenylic position have a small activation barrier of 9.1 kcal/mol, and it may arise from the required geometric distortion or charge separation. Moreover, this process shows no significant solvent polarity dependence, consistent with the absence of the polar electronic state during the addition behaviour. Combination with the previous study of MARACA, a clear description of the reactivity of  $\alpha,3$ -dehydrotoluene diradicals produced from cycloaromatization was presented, which will be beneficial for deeper understanding in diradical chemistry and guide the molecular design for novel enediyne antibiotics.

## Experimental Section

**General methods.** Toluene and tetrahydrofuran (THF) were dried over calcium hydride ( $\text{CaH}_2$ ) and distilled prior to use. Deuterated alcohol ( $\text{CD}_3$ )<sub>2</sub>CDOH was prepared from ( $\text{CD}_3$ )<sub>2</sub>CDOD according to a literature procedure.<sup>[40]</sup> Other reagents were purchased at commercial grade and used without further purification. Sonogashira coupling reactions were performed with dry Schlenk techniques under an atmosphere of nitrogen. <sup>1</sup>H NMR and <sup>13</sup>C{<sup>1</sup>H} NMR spectra were recorded on Bruker DRX-500 or DRX-600 instruments and calibrated using residual undeuterated solvent ( $\text{CDCl}_3$ :  $\delta_{\text{H}} = 7.26$  ppm,  $\delta_{\text{C}} = 77.2$  ppm) as an internal reference. High resolution mass spectra (HR-MS) were obtained on a Micromass LCTM mass spectrometer using the ESI method (electrospray ionization). Reactions were monitored by thin-layer chromatography (TLC).

Typical procedure for the synthesis of *tert*-butyl 2-(4-(2-((*tert*-butoxycarbonyl)(*tert*-butyl)amino)ethyl)-3-(*tert*-butyl)-2,5,7-trioxo-2,3,5,7-tetrahydro-6*H*-oxazolo[4,5-*f*]isindol-6-yl)acetate (**2**) from the tandem Sonogashira coupling/cyclization reaction. 3,4-diiodomaleimide<sup>[28]</sup> **1a** (231.4 mg, 0.5 mmol), CuI (38.1 mg, 40%), ( $\text{PPh}_3$ )<sub>2</sub>PdCl<sub>2</sub> (35.1 mg, 10%), and diisopropylethyl amine (DIPEA, 261  $\mu\text{L}$ , 1.5 mmol) were successively added to dry toluene (4 mL) under nitrogen. After that, a solution of terminal alkyne **1b** (316.6 mg, 1.5 mmol) in THF (1 mL) was added dropwise, and the reaction system was stirred at room temperature for 24 h. After the completion of the reaction as detected by TLC, purification of the crude product by column chromatography on silica gel (eluent: hexane/ethyl acetate = 15:1 ~ 8:1) was conducted to afford both enediyne compound **1** as a yellow oil (46 mg, 15%) and cyclized product **2** as a yellow solid (34 mg, 12%). All spectroscopic data were in agreement with that in previous work.<sup>[28]</sup>

**General procedure for the synthesis of deuterium labeled **2** using different additives.** Based on the procedure mentioned above for the synthesis of compound **2**, various deuterated agents were added together with the terminal alkyne. To gain a relatively thorough transformation from compound **1** to **2** in this cascade reaction, the minor modification of the prolonged reaction time (32 ~ 48 h) were adopted. After the completion of the reaction

monitored by TLC, the resulted mixture was directly purified by column chromatography on silica gel (eluent: hexane/ethyl acetate = 8:1) to give the product.

Additives:  $\text{CD}_3\text{OD}$  (203  $\mu\text{L}$ , 5 mmol) and  $\text{D}_2\text{O}$  (36  $\mu\text{L}$ , 2 mmol). Isolated as a yellow solid (46 mg, 16%). <sup>1</sup>H NMR (500 MHz,  $\text{CDCl}_3$ )  $\delta$  7.46 (s, 0.32H), 4.30 (s, 2H), 3.60 (t,  $J = 6.4$  Hz, 1.06H), 3.51–3.40 (m, 2H), 1.75 (s, 9H), 1.46 (s, 9H), 1.37 (s, 9H), 1.31 (s, 9H); <sup>13</sup>C{<sup>1</sup>H} NMR (151 MHz,  $\text{CDCl}_3$ )  $\delta$  168.2, 166.7, 166.5, 156.1, 153.5, 147.8, 136.0, 128.4, 127.1, 126.0, 103.4, 83.0, 80.1, 60.6, 55.9, 46.3, 39.9, 34.2 (t,  $J = 19.9$  Hz), 30.2, 30.0, 28.6, 28.2; HRMS (ESI-TOF)  $m/z$ :  $[\text{M} + \text{Na}]^+$  calcd for  $\text{C}_{30}\text{H}_{43}\text{N}_3\text{O}_8\text{Na}$  596.2948; found 596.2937 ( $[\text{D}_0\text{J}-2$ ]);  $[\text{M} + \text{Na}]^+$  calcd for  $\text{C}_{30}\text{H}_{42}\text{DN}_3\text{O}_8\text{Na}$  597.3011; found 597.3011 ( $[\text{D}_1\text{J}-2$ ]);  $[\text{M} + \text{Na}]^+$  calcd for  $\text{C}_{30}\text{H}_{41}\text{D}_2\text{N}_3\text{O}_8\text{Na}$  598.3073; found 598.3072 ( $[\text{D}_2\text{J}-2$ ]);  $[\text{M} + \text{Na}]^+$  calcd for  $\text{C}_{30}\text{H}_{40}\text{D}_3\text{N}_3\text{O}_8\text{Na}$  599.3136; found 599.3107 ( $[\text{D}_3\text{J}-2$ ]).

Additives:  $\text{CH}_3\text{OD}$  (203  $\mu\text{L}$ , 5 mmol) and  $\text{D}_2\text{O}$  (36  $\mu\text{L}$ , 2 mmol). Isolated as a yellow solid (53 mg, 18%). <sup>1</sup>H NMR (500 MHz,  $\text{CDCl}_3$ )  $\delta$  7.46 (s, 0.33H), 4.29 (s, 2H), 3.59 (t,  $J = 6.5$  Hz, 1.08H), 3.51–3.37 (m, 2H), 1.75 (s, 9H), 1.45 (s, 9H), 1.37 (s, 9H), 1.31 (s, 9H); <sup>13</sup>C{<sup>1</sup>H} NMR (151 MHz,  $\text{CDCl}_3$ )  $\delta$  168.2, 166.7, 166.5, 156.0, 153.4, 147.7, 136.0, 128.4, 127.1, 126.0, 103.4, 83.0, 80.1, 60.6, 55.8, 46.3, 39.9, 34.2 (t,  $J = 19.9$  Hz), 30.2, 30.0, 28.6, 28.1; HRMS (ESI-TOF)  $m/z$ :  $[\text{M} + \text{Na}]^+$  calcd for  $\text{C}_{30}\text{H}_{43}\text{N}_3\text{O}_8\text{Na}$  596.2948; found 596.2963 ( $[\text{D}_0\text{J}-2$ ]);  $[\text{M} + \text{Na}]^+$  calcd for  $\text{C}_{30}\text{H}_{42}\text{DN}_3\text{O}_8\text{Na}$  597.3011; found 597.3019 ( $[\text{D}_1\text{J}-2$ ]);  $[\text{M} + \text{Na}]^+$  calcd for  $\text{C}_{30}\text{H}_{41}\text{D}_2\text{N}_3\text{O}_8\text{Na}$  598.3073; found 598.3074 ( $[\text{D}_2\text{J}-2$ ]);  $[\text{M} + \text{Na}]^+$  calcd for  $\text{C}_{30}\text{H}_{40}\text{D}_3\text{N}_3\text{O}_8\text{Na}$  599.3136; found 599.3123 ( $[\text{D}_3\text{J}-2$ ]).

Additives:  $\text{CH}_3\text{OD}$  (203  $\mu\text{L}$ , 5 mmol). Isolated as a yellow solid (53 mg, 18%). <sup>1</sup>H NMR (500 MHz,  $\text{CDCl}_3$ )  $\delta$  7.45 (s, 0.39H), 4.29 (s, 2H), 3.59 (t,  $J = 6.5$  Hz, 1.24H), 3.50–3.38 (m, 2H), 1.74 (s, 9H), 1.45 (s, 9H), 1.36 (s, 9H), 1.30 (s, 9H); <sup>13</sup>C{<sup>1</sup>H} NMR (151 MHz,  $\text{CDCl}_3$ )  $\delta$  168.2, 166.7, 166.5, 156.0, 153.4, 147.7, 136.0, 128.4, 127.1, 126.0, 103.4, 83.0, 80.0, 60.6, 55.8, 46.3, 39.9, 34.1 (t,  $J = 19.9$  Hz), 30.2, 30.0, 28.6, 28.1; HRMS (ESI-TOF)  $m/z$ :  $[\text{M} + \text{Na}]^+$  calcd for  $\text{C}_{30}\text{H}_{43}\text{N}_3\text{O}_8\text{Na}$  596.2948; found 596.2958 ( $[\text{D}_0\text{J}-2$ ]);  $[\text{M} + \text{Na}]^+$  calcd for  $\text{C}_{30}\text{H}_{42}\text{DN}_3\text{O}_8\text{Na}$  597.3011; found 597.3013 ( $[\text{D}_1\text{J}-2$ ]);  $[\text{M} + \text{Na}]^+$  calcd for  $\text{C}_{30}\text{H}_{41}\text{D}_2\text{N}_3\text{O}_8\text{Na}$  598.3073; found 598.3072 ( $[\text{D}_2\text{J}-2$ ]);  $[\text{M} + \text{Na}]^+$  calcd for  $\text{C}_{30}\text{H}_{40}\text{D}_3\text{N}_3\text{O}_8\text{Na}$  599.3136; found 599.3116 ( $[\text{D}_3\text{J}-2$ ]).

Additives:  $\text{CD}_3\text{OH}$  (203  $\mu\text{L}$ , 5 mmol) and  $\text{H}_2\text{O}$  (36  $\mu\text{L}$ , 2 mmol). Isolated as a yellow solid (32 mg, 11%). <sup>1</sup>H NMR (600 MHz,  $\text{CDCl}_3$ )  $\delta$  7.46 (s, 1H), 4.30 (s, 2H), 3.60 (t,  $J = 6.5$  Hz, 2H), 3.46 (t,  $J = 6.5$  Hz, 2H), 1.75 (s, 9H), 1.46 (s, 9H), 1.37 (s, 9H), 1.32 (s, 9H); <sup>13</sup>C{<sup>1</sup>H} NMR (151 MHz,  $\text{CDCl}_3$ )  $\delta$  168.2, 166.7, 166.5, 156.1, 153.5, 147.8, 136.0, 128.5, 127.2, 126.1, 103.4, 83.0, 80.1, 60.6, 55.9, 46.4, 40.0, 34.2, 30.2, 30.0, 28.6, 28.2; HRMS (ESI-TOF)  $m/z$ :  $[\text{M} + \text{Na}]^+$  calcd for  $\text{C}_{30}\text{H}_{43}\text{N}_3\text{O}_8\text{Na}$  596.2948; found 596.2949 ( $[\text{D}_0\text{J}-2$ ]).

Additives: ( $\text{CD}_3$ )<sub>2</sub>CDOD (383  $\mu\text{L}$ , 5 mmol) and  $\text{D}_2\text{O}$  (36  $\mu\text{L}$ , 2 mmol). Isolated as a yellow solid (36 mg, 12%). <sup>1</sup>H NMR (600 MHz,  $\text{CDCl}_3$ )  $\delta$  7.47 (s, 0.31H), 4.30 (s, 2H), 3.60 (t,  $J = 6.5$  Hz, 1.03H), 3.50–3.41 (m, 2H), 1.75 (s, 9H), 1.46 (s, 9H), 1.38 (s, 9H), 1.32 (s, 9H); <sup>13</sup>C{<sup>1</sup>H} NMR (151 MHz,  $\text{CDCl}_3$ )  $\delta$  168.2, 166.7, 166.5, 156.1, 153.5, 147.8, 136.1, 128.4, 127.2, 126.1, 103.4, 83.0, 80.1, 60.6, 55.9, 46.3, 40.0, 34.2 (t,  $J = 19.9$  Hz), 30.2, 30.0, 28.6, 28.2; HRMS (ESI-TOF)  $m/z$ :  $[\text{M} + \text{Na}]^+$  calcd for  $\text{C}_{30}\text{H}_{43}\text{N}_3\text{O}_8\text{Na}$  596.2948; found 596.2958 ( $[\text{D}_0\text{J}-2$ ]);  $[\text{M} + \text{Na}]^+$  calcd for  $\text{C}_{30}\text{H}_{42}\text{DN}_3\text{O}_8\text{Na}$  597.3011; found 597.3019 ( $[\text{D}_1\text{J}-2$ ]);  $[\text{M} + \text{Na}]^+$  calcd for  $\text{C}_{30}\text{H}_{41}\text{D}_2\text{N}_3\text{O}_8\text{Na}$  598.3073; found 598.3074 ( $[\text{D}_2\text{J}-2$ ]);  $[\text{M} + \text{Na}]^+$  calcd for  $\text{C}_{30}\text{H}_{40}\text{D}_3\text{N}_3\text{O}_8\text{Na}$  599.3136; found 599.3124 ( $[\text{D}_3\text{J}-2$ ]).

Additives: ( $\text{CD}_3$ )<sub>2</sub>CDOH (383  $\mu\text{L}$ , 5 mmol) and  $\text{H}_2\text{O}$  (36  $\mu\text{L}$ , 2 mmol). Isolated as a yellow solid (31 mg, 11%) from the general procedure for the synthesis of deuterium labeled  $[\text{D}_0\text{J}-2$ . <sup>1</sup>H NMR (600 MHz,  $\text{CDCl}_3$ )  $\delta$  7.47 (s, 1H), 4.30 (s, 2H), 3.60 (t,  $J = 6.5$  Hz, 2H), 3.46 (t,  $J = 6.5$  Hz, 2H), 1.75 (s, 9H), 1.46 (s, 9H), 1.38 (s, 9H), 1.32 (s, 9H); <sup>13</sup>C{<sup>1</sup>H} NMR (151 MHz,  $\text{CDCl}_3$ )  $\delta$  168.2, 166.7, 166.5, 156.1, 153.5, 147.8, 136.1, 128.5, 127.2, 126.1, 103.4, 83.0, 80.1, 60.7, 55.9, 46.4, 40.0,

34.2, 30.2, 30.0, 28.6, 28.2; HRMS (ESI-TOF) m/z:  $[M + Na]^+$  calcd for  $C_{30}H_{43}N_3O_8Na$  596.2948; found 596.2949 ( $[D_0]^-2$ ).

## Acknowledgements

Dedicated to the 100th anniversary of Chemistry at Nankai University. The authors gratefully acknowledge the financial support from National Natural Science Foundation of China (21871080, 21503078), Natural Science Foundation of Shanghai (20ZR1413400), the Fundamental Research Funds for the Central Universities (22221818014), and Shanghai Leading Academic Discipline Project (B502). AH thanks the "Eastern Scholar Professorship" support from Shanghai local government.

## Conflict of Interest

The authors declare no conflict of interest.

**Keywords:** Acyclic enediyne · Cycloaromatization · Nucleophilic addition · Diradicals · Zwitterions

- [1] a) R. R. Jones, R. G. Bergman, *J. Am. Chem. Soc.* **1972**, *94*, 660–661; b) R. G. Bergman, *Acc. Chem. Res.* **1973**, *6*, 25–31; c) T. P. Lockhart, P. B. Comita, R. G. Bergman, *J. Am. Chem. Soc.* **1981**, *103*, 4082–4090.
- [2] a) A. G. Myers, E. Y. Kuo, N. S. Finney, *J. Am. Chem. Soc.* **1989**, *111*, 8057–8059; b) A. G. Myers, P. S. Dragovich, E. Y. Kuo, *J. Am. Chem. Soc.* **1992**, *114*, 9369–9386; c) A. G. Myers, P. S. Dragovich, *J. Am. Chem. Soc.* **1989**, *111*, 9130–9132.
- [3] R. K. Mohamed, P. W. Peterson, I. V. Alabugin, *Chem. Rev.* **2013**, *113*, 7089–7129.
- [4] a) J. W. Grissom, G. U. Gunawardena, D. Klingberg, D. Huang, *Tetrahedron* **1996**, *52*, 6453–6518; b) C. Raviola, S. Protti, D. Ravelli, M. Fagnoni, *Chem. Soc. Rev.* **2016**, *45*, 4364–4390.
- [5] U. Galm, M. H. Hager, S. G. Van Lanen, J. Ju, J. S. Thorson, B. Shen, *Chem. Rev.* **2005**, *105*, 739–758.
- [6] a) J. P. Johnson, D. A. Bringley, E. E. Wilson, K. D. Lewis, L. W. Beck, A. J. Matzger, *J. Am. Chem. Soc.* **2003**, *125*, 14708–14709; b) S. Chen, A. Hu, *Sci. China Chem.* **2015**, *58*, 1710–1723.
- [7] M. D. Lee, T. S. Dunne, C. C. Chang, G. A. Ellestad, M. M. Siegel, G. O. Morton, W. J. McGahren, D. B. Borders, *J. Am. Chem. Soc.* **1987**, *109*, 3466–3468.
- [8] M. Konishi, H. Ohkuma, K. Matsumoto, T. Tsuno, H. Kamei, T. Miyaki, T. Oki, H. Kawaguchi, G. D. Vanduyne, J. Clardy, *J. Antibiot.* **1989**, *42*, 1449–1452.
- [9] J. Golik, J. Clardy, G. Dubay, G. Groenewold, H. Kawaguchi, M. Konishi, B. Krishnan, H. Ohkuma, K. Saitoh, T. W. Doyle, *J. Am. Chem. Soc.* **1987**, *109*, 3461–3462.
- [10] C.-Y. Chang, X. Yan, I. Crnovic, T. Annaval, C. Chang, B. Nocek, J. D. Rudolf, D. Yang, Hindra, G. Babnigg, A. Joachimiak, G. N. Phillips, B. Shen, *Cell Chem. Biol.* **2018**, *25*, 1075–1085.e1074.
- [11] N. Ishida, K. Miyazaki, K. Kumagai, M. Rikimaru, *J. Antibiot. Ser. A* **1965**, *18*, 68–76.
- [12] C. Vavilala, N. Byrne, C. M. Kraml, D. M. Ho, R. A. Pascal, *J. Am. Chem. Soc.* **2008**, *130*, 13549–13551.
- [13] M. Schmittel, M. Strittmatter, S. Kiau, *Angew. Chem. Int. Ed. Engl.* **1996**, *35*, 1843–1845.
- [14] S. Braverman, D. Segev, *J. Am. Chem. Soc.* **1974**, *96*, 1245–1247.
- [15] H. Hopf, H. Musso, *Angew. Chem. Int. Ed. Engl.* **1969**, *8*, 680–680.
- [16] J. O. Karlsson, V. N. Nghi, L. D. Foland, H. W. Moore, *J. Am. Chem. Soc.* **1985**, *107*, 3392–3393.
- [17] P. W. Peterson, R. K. Mohamed, I. V. Alabugin, *Eur. J. Org. Chem.* **2013**, *2013*, 2505–2527.
- [18] G. dos Passos Gomes, I. V. Alabugin, *J. Am. Chem. Soc.* **2017**, *139*, 3406–3416.
- [19] C. Pedroli, D. Ravelli, S. Protti, A. Albini, M. Fagnoni, *J. Org. Chem.* **2017**, *82*, 6592–6603.
- [20] a) T. P. Goncalves, M. Mohamed, R. J. Whitby, H. F. Sneddon, D. C. Harrowven, *Angew. Chem. Int. Ed.* **2015**, *54*, 4531–4534; *Angew. Chem.* **2015**, *127*, 4614–4617; b) H. Li, H. Yang, J. L. Petersen, K. K. Wang, *J. Org. Chem.* **2004**, *69*, 4500–4508.
- [21] T. S. Hughes, B. K. Carpenter, *J. Chem. Soc. Perkin Trans. 2* **1999**, 2291–2298.
- [22] a) M. E. Cremeens, T. S. Hughes, B. K. Carpenter, *J. Am. Chem. Soc.* **2005**, *127*, 6652–6661; b) B. K. Carpenter, *Chem. Soc. Rev.* **2006**, *35*, 736–747.
- [23] C. L. Perrin, B. L. Rodgers, J. M. O'Connor, *J. Am. Chem. Soc.* **2007**, *129*, 4795–4799.
- [24] a) E. Das, S. Basak, A. Anoop, A. Basak, *J. Org. Chem.* **2018**, *83*, 7730–7740; b) E. Das, S. Basak, A. Anoop, S. Chand, A. Basak, *J. Org. Chem.* **2019**, *84*, 2911–2921.
- [25] P. G. Wenthold, A. H. Winter, *J. Org. Chem.* **2018**, *83*, 12390–12396.
- [26] P. G. Wenthold, A. H. Winter, *J. Org. Chem.* **2018**, *83*, 12397–12403.
- [27] a) D. Song, S. Sun, Y. Tian, S. Huang, Y. Ding, Y. Yuan, A. Hu, *J. Mater. Chem. B* **2015**, *3*, 3195–3200; b) H. Lu, H. Ma, B. Li, M. Zhang, H. Chen, Y. Wang, X. Li, Y. Ding, A. Hu, *J. Mater. Chem. B* **2020**, *8*, 1971–1979; c) B. Li, B. Duan, J. Li, M. Zhang, Y. Yuan, Y. Ding, A. Hu, *Tetrahedron* **2018**, *74*, 6419–6425; d) H. Chen, B. Li, M. Zhang, H. Lu, Y. Wang, W. Wang, Y. Ding, A. Hu, *ChemistrySelect* **2020**, *5*, 7069–7075; e) Y. Wang, B. Li, M. Zhang, H. Lu, H. Chen, W. Wang, Y. Ding, A. Hu, *Tetrahedron* **2020**, *76*, 131242.
- [28] M. Zhang, B. Li, H. Chen, H. Lu, H. Ma, X. Cheng, W. Wang, Y. Wang, Y. Ding, A. Hu, *J. Org. Chem.* **2020**, *85*, 9808–9819.
- [29] a) H. Lu, M. Zhang, B. Li, H. Ma, W. Wang, Y. Ding, X. Li, A. Hu, *Asian J. Org. Chem.* **2020**, *9*, 2170–2175; b) M. Zhang, H. Lu, B. Li, H. Ma, W. Wang, X. Cheng, Y. Ding, A. Hu, *J. Org. Chem.* **2021**, *86*, 1549–1559.
- [30] a) M. J. S. Dewar, S. Kirschner, H. W. Kollmar, L. E. Wade, *J. Am. Chem. Soc.* **1974**, *96*, 5242–5244; b) M. Balci, W. M. Jones, *J. Am. Chem. Soc.* **1980**, *102*, 7607–7608.
- [31] W. Adcock, C. P. Andrieux, C. I. Clark, A. Neudeck, J.-M. Saveant, C. Tardy, *J. Am. Chem. Soc.* **1995**, *117*, 8285–8286.
- [32] a) C. L. Perrin, G. J. Reyes-Rodríguez, *J. Am. Chem. Soc.* **2014**, *136*, 15263–15269; b) S. D. Chen, S. Huang, C. G. Wang, Y. Ding, A. G. Hu, *Asian J. Org. Chem.* **2017**, *6*, 1099–1103.
- [33] a) P. Hohenberg, W. Kohn, *Phys. Rev. B.* **1964**, *136*, 864–871; b) W. Kohn, L. J. Sham, *Phys. Rev.* **1965**, *140*, A1133–A1138.
- [34] M. J. Frisch, G. W. Trucks, H. B. Schlegel, G. E. Scuseria, M. A. Robb, J. R. Cheeseman, G. Scalmani, V. Barone, B. Mennucci, G. A. Petersson, H. Nakatsuji, M. Caricato, X. Li, H. P. Hratchian, A. F. Izmaylov, J. Bloino, G. Zheng, J. L. Sonnenberg, M. Hada, M. Ehara, K. Toyota, R. Fukuda, J. Hasegawa, M. Ishida, T. Nakajima, Y. Honda, O. Kitao, H. Nakai, T. Vreven, J. A. Montgomery Jr., J. E. Peralta, F. Ogliaro, M. Bearpark, J. J. Heyd, E. Brothers, K. N. Kudin, V. N. Staroverov, R. Kobayashi, J. Normand, K. Raghavachari, A. Rendell, J. C. Burant, S. S. Iyengar, J. Tomasi, M. Cossi, N. Rega, J. M. Millam, M. Klene, J. E. Knox, J. B. Cross, V. Bakken, C. Adamo, J. Jaramillo, R. Gomperts, R. E. Stratmann, O. Yazyev, A. J. Austin, R. Cammi, C. Pomelli, J. W. Ochterski, R. L. Martin, K. Morokuma, V. G. Zakrzewski, G. A. Voth, P. Salvador, J. J. Dannenberg, S. Dapprich, A. D. Daniels, Ö. Farkas, J. B. Foresman, J. V. Ortiz, J. Cioslowski, D. J. Fox in *Gaussian 09, Revision E.01*, Vol. Gaussian, Inc.: Wallingford CT, **2009**.
- [35] a) A. Basak, S. Das, D. Mallick, E. D. Jemmis, *J. Am. Chem. Soc.* **2009**, *131*, 15695–15704; b) I. V. Alabugin, M. Manoharan, *J. Am. Chem. Soc.* **2003**, *125*, 4495–4509.
- [36] M. Cossi, G. Scalmani, N. Rega, V. Barone, *J. Chem. Phys.* **2002**, *117*, 43–54.
- [37] J. M. Saveant, *J. Phys. Chem.* **1994**, *98*, 3716–3724.
- [38] Q. N. N. Nguyen, D. J. Tantillo, *J. Org. Chem.* **2016**, *81*, 5295–5302.
- [39] a) C. Raviola, D. Ravelli, S. Protti, M. Fagnoni, *J. Am. Chem. Soc.* **2014**, *136*, 13874–13881; b) I. Suzuki, A. Shigenaga, A. Manabe, H. Nemoto, M. Shibuya, *Tetrahedron* **2003**, *59*, 5691–5704.
- [40] C. P. Casey, J. B. Johnson, *J. Org. Chem.* **2003**, *68*, 1998–2001.

Manuscript received: February 23, 2021  
Revised manuscript received: March 31, 2021  
Accepted manuscript online: April 1, 2021  
Version of record online: May 1, 2021